Decoupled Trajectory Planning for Monitoring UAVs and UGV Carrier by Reachable Sets

Kim, Taewan; Vinod, Abraham P.; Di Cairano, Stefano

TR2024-092 July 09, 2024

Abstract

We consider the trajectory generation for a UGV and multiple UAVs that are tasked with monitoring certain specified target areas, where the former carries and re-charges the latter ones. We decouple the motion planning of UGVs and UAVs using reachable sets constructed from Lyapunov functions. The reachable sets are used as constraints for UGV trajectory generation resulting in existence guarantees of feasible UAVs trajectories with respect to flight and energy constraints. The reachable sets also provide an initial trajectory for UAVs rendezvous from and launch to the targets, which may be refined by optimization. We show simulation results of a case study with multiple UAVs monitoring multiple target sites.

American Control Conference (ACC) 2024

Decoupled Trajectory Planning for Monitoring UAVs and UGV Carrier by Reachable Sets

Taewan Kim, Abraham P. Vinod and Stefano Di Cairano

Abstract— **We consider the trajectory generation for a UGV and multiple UAVs that are tasked with monitoring certain specified target areas, where the former carries and re-charges the latter ones. We decouple the motion planning of UGVs and UAVs using reachable sets constructed from Lyapunov functions. The reachable sets are used as constraints for UGV trajectory generation resulting in existence guarantees of feasible UAVs trajectories with respect to flight and energy constraints. The reachable sets also provide an initial trajectory for UAVs rendezvous from and launch to the targets, which may be refined by optimization. We show simulation results of a case study with multiple UAVs monitoring multiple target sites.**

I. Introduction

Coordinated operation of heterogeneous autonomous vehicles, such as unmanned ground and aerial vehicles (UGVs and UAVs, respectively) may automate many tasks that are time consuming, expensive, and tiring or dangerous for humans. One such tasks is monitoring [1] of distributed infrastructure, such as power lines, gas and oil pipelines, and of the environment, such as forests, water networks and farming areas, for preventive maintenance and risk mitigation. Monitoring often requires operating in remote or impervious areas, possibly for long periods of time, and the amount of collected information on the targets usually depends on how and for how long the targets are monitored.

Here, we consider motion planning for an UGV and multiple UAVs to monitor a sequence of targets. The plans of UGV and UAVs are correlated because the UAVs depart from and rendezvous with the UGV for long distance transport, re-charging, and possibly data dumping. Thus, while the UGV does not need to visit the targets itself, it needs to follow a plan that allows for recovery of UAV within the battery range and in a suitable time interval.

Even when the sequence of targets is assigned, e.g., by [2], and the references therein, the UGV and UAV planning problem presents multiple challenges: (i) the time scales, ranges, and capabilities of UGV and UAVs are significantly different; (ii) the computational resources required to solve the problem increase with the number of UAVs; (iii) for determining the UAV range, the energy consumption during flight can be estimated precisely given the flight profile, but the time and energy consumption during information acquisition and transmission, which are significant for small UAVs, are hard to predict.

Taewan Kim is with the Dep. Aeronautics and Astronautics, University of Washington, Seattle, WA (email:twankim@uw.edu). He was an intern at MERL during this work.

A.P. Vinod and S. Di Cairano are with Mitsubishi Electric Research Laboratories, Cambridge, MA (email:dicairano@ieee.org, vinod@merl.com)

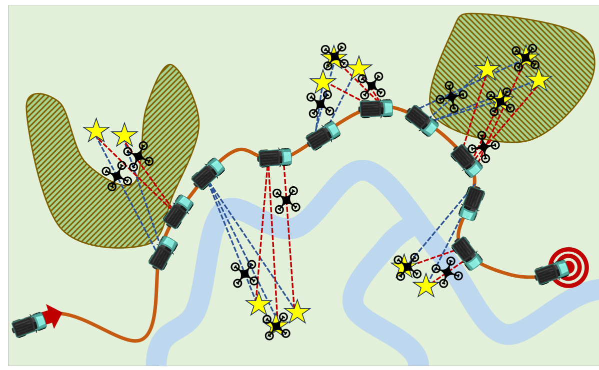

Fig. 1. Scenario of monitoring by UGV carrying multiple UAVs. Targets (stars), non-traversable terrain (green-brown), non-crossable river (blue), UGV path (orange), UAV launch (blue) and return (red) paths. UGV and UAVs positions shown at different time instants.

In recent years [3], coordination of UGVs and UAVs is becoming an active research area. Prior research on coordinating task-executing UAVs with re-charging UGVs, see, e.g., [3]–[7] focuses on grid environments, uses graphs methods, e.g., the generalized traveling salesman problem (GTSP), by discretizing the space, and often ignores the UAVs and UGVs dynamics and constraints. The UGV is often considered only as a mobile charging station, and the energy/range depletion models are usually perfectly known.

In this work we consider the generation of trajectories for an UGV carrying and re-charging multiple UAVs tasked with acquiring monitoring information from multiple targets. We account for UGV and UAVs dynamics and operational constraints. We only use an UAV energy depletion model during flight, because during monitoring the energy consumption depends on sensing and transmission and is hard to predict. Since we do not rely on energy consumption models during monitoring and to address time-scale separation and computational burden, we decouple the UGV and UAV trajectory generation while ensuring satisfaction of constraints, energy budget, and rendezvous using reachable sets constructed from sublevel sets of Lyapunov functions [8]. The obtained UAV launch and recovery trajectories may be further refined by separately optimizing each one.

In what follows, Section II formulates the planning problem, Section III designs constraints that ensure feasible UGV-UAV rendezvous, Section IV and Section V describe UGV trajectory generation and optimization of each UAV launch and recovery trajectories, respectively. Section VI reports a case study and Section VII summarizes the conclusions.

Notation: $\mathbb{R}$ ($\mathbb{Z}$), $\mathbb{R}_{0+}$ ($\mathbb{Z}_{0+}$), $\mathbb{R}_{+}$ ($\mathbb{Z}_{+}$) are the sets of real (integer), nonnegative real (integer), positive real (integer) numbers. Intervals are denoted by $\mathbb{Z}_{[a,b)} = \{z \in \mathbb{Z} : a \leq z < b\}$, I is the identity matrix, 0 an "all-zeros" matrix of appropriate dimensions, and $Q \succ 0$, ($Q \succeq 0$), a positive (semi) definite matrix. For vectors x, y, the stacking is $(x, y) = [x^\top \; y^\top]^\top$. We denote the 2-norm by $\|\cdot\|$.

II. Modeling and Problem Formulation

We consider the motion planning of one UGV, with state vector $x_g \in \mathbb{R}^{n_g}$, and N_a UAVs, with state vectors $x_a^{(i)} \in \mathbb{R}^{n_a}$, $i \in \mathbb{Z}_{[1,N_a]}$. The UGV motion model is

$$\dot{x}_g(t) = f_g(x_g(t), u_g(t)) \tag{1a}$$
$$p_g(t) = h_g(x_g(t)), \tag{1b}$$

where $u_g \in \mathbb{R}^{m_g}$ is the input vector and $p_g \in \mathbb{R}^2$ is the position vector in global coordinates. The choices for the UGV motion model include linear double integrators, unicycle, and bicycle. The UGV is subject to constraints

$$x_g \in \mathcal{X}_g, \quad u_g \in \mathcal{U}_g, \tag{2}$$

where $\mathcal{X}_g \subseteq \mathbb{R}^{n_g}$, $\mathcal{U}_g \subseteq \mathbb{R}^{m_g}$, are sets defining the admissible state and input vectors, respectively.

We consider quadrotor UAVs with linear motion model

$$\dot{x}_a^{(i)}(t) = Ax_a^{(i)}(t) + Bu_a^{(i)}(t), \tag{3a}$$
$$p_a^{(i)}(t) = Cx_a^{(i)}(t), \tag{3b}$$

where $u_a^{(i)} \in \mathbb{R}^{m_a}$ is the input vector and $p_a^{(i)} \in \mathbb{R}^2$ is the UAV position vector in global coordinates, for all $i \in \mathbb{Z}_{[1,N_a]}$. Here, (3) consists of two double integrators, $n_a = 4$, $m_a = 2$,

$$A = \begin{bmatrix} 0 & I \\ 0 & 0 \end{bmatrix}, \quad B = \begin{bmatrix} 0 \\ I \end{bmatrix}, \quad C = \begin{bmatrix} I & 0 \end{bmatrix},$$

and $x_a^{(i)} = [p_{a,x}^{(i)}, p_{a,y}^{(i)}, v_{a,x}^{(i)}, v_{a,y}^{(i)}]^\top$, $u_a^{(i)} = [a_{a,x}^{(i)}, a_{a,y}^{(i)}]^\top$. For shortness, $p_a^{(i)} = (p_{a,x}^{(i)}, p_{a,y}^{(i)})$, $v_a^{(i)} = (v_{a,x}^{(i)}, v_{a,y}^{(i)})$, and $a_a^{(i)} = (a_{a,x}^{(i)}, a_{a,y}^{(i)})$ denote the position, velocity and acceleration vectors, respectively. The UAVs are subject to constraints on velocity and acceleration, $\|v_a^{(i)}\| \leq v_{\max}$, $\|a_a\|^{(i)} \leq a_{\max}$, for all $i \in \mathbb{Z}_{[1,N_a]}$ that can be written as

$$x_a^{(i)} \in \mathcal{X}_a, \quad u_a^{(i)} \in \mathcal{U}_a, \tag{4}$$

where $\mathcal{X}_a \subseteq \mathbb{R}^{n_a}, \mathcal{U}_g \subseteq \mathbb{R}^{m_a}$ are the sets of admissible UAVs state and input vectors, respectively. Here, we consider the UAVs to be faster than the UGV.

Remark 1. *For simplicity, we model the motion of the UAVs in 2D, i.e., with a constant flight altitude, but all out developments translate immediately to the 3D case, where a third integrator is added for the altitude dynamics.*

The range of the UGV is assumed to be significantly longer than what needed for the task to be executed, while the UAVs are battery powered and have limited range. For energy consumption during flight, the spent battery energy changes according to $\dot{\mathcal{E}}(t) = c_2(v_a^{(i)}(t))^2 + c_1(a_a^{(i)}(t))^2$, where we model the dominant effects of airdrag as proportional to the square of the velocity, and losses, mechanical and electrical, in accelerating as proportional to the squared acceleration. Thus, the consumed energy evolves as

$$\dot{\mathcal{E}}^{(i)}(t) = x_a^{(i)}(t)^\top Q_e x_a^{(i)}(t) + u_a^{(i)}(t)^\top R_e u_a^{(i)}(t), \tag{5}$$

and the energy capacity constraint $\mathcal{E}^{(i)}(t)^{(i)} \leq \mathcal{E}_{\max}$ for $i \in \mathbb{Z}_{[1,N_a]}$ must be satisfied, where $\mathcal{E}_{\max}$ is the maximum usable energy. During monitoring operation, a major source of energy consumption is due to sensors, from processing acquired information, and possibly from communicating data to the UGV acting as base station. A prediction model for such consumption is hard to develop, and hence here we do not rely on it, as it will become clear later.

Remark 2. *In model* (5) *we are ignoring the idling and stationary flight energy consumption, since we focus on the mission phases when the UAVs are moving. These may be included as constants or ignored if we allow the UAV to land and stop the propellers.*

While the UAV has limited range, it is unaffected by ground obstacles, which impose constraints on the UGV. The exclusion constraints on the UGV are

$$p_g \notin \mathcal{O}^{(o)}, o \in \mathbb{Z}_{[1,N_O]}, \tag{6}$$

where N_o is the number of obstacles, and $\mathcal{O}^{(o)}$ is the collision region for obstacle o, i.e., the set of UGV positions p_g for which a collision may occur, accounting for the physical shapes of both, obstacle and UGV.

The objective of the UGV and UAVs is to acquire information about a set of targets, $j \in \mathbb{Z}_{[1,N_m]}$ located a known positions $p_m^{(j)} = (p_{m,x}^{(j)}, p_{m,y}^{(j)})$. For that the UGV releases the UAVs carrying the sensors and communication to fly at the monitoring location, acquire data with sensors, process them and send the raw and/or processed data back to the UGV for storage or long distance transmission. We assume that the sequence in which targets are to be visited is assigned, e.g., by [2], and are clustered in groups with know maximum number of elements per cluster.

Problem 1. *Given initial time instant T_0, N_m monitoring targets with positions $p_m^{(j)} = (p_{m,x}^{(j)}, p_{m,y}^{(j)})$, $j \in \mathbb{Z}_{[1,N_m]}$, N_O obstacle collision sets $\mathcal{O}^{(o)} \subseteq \mathbb{R}^2$, $o \in \mathbb{Z}_{[1,N_O]}$, a UGV with motion model* (1) *subject to* (2), (6), *initial state $x_g(T_0) = x_{g,s}$ and desired final state $x_{g,f}$, and N_a UAVs with motion model* (3), *energy depletion model* (5), *subject to* (4) *and initial states $x_{a,s}^{(i)} = x_{g,s}$ for $i \in \mathbb{Z}_{[1,N_a]}$, determine*

i) a terminal time instant $T_f > T_0$

ii) time instants $t_{i,j}^l$, $t_{i,j}^b$, $t_{i,j}^e$, $t_{i,j}^r$, $j \in \mathbb{Z}_{[1,N_m]}$, $i \in \mathbb{Z}_{[1,N_a]}$,

iii) commands $u_g(t)$ for $t \in [T_0, T_f]$, $u_a^{(i)}(t)$ for $t \in \bigcup_{j=1}^{N_m}[t_{i,j}^l, t_{i,j}^b] \cup [t_{i,j}^e, t_{i,j}^r]$, $i \in \mathbb{Z}_{[1,N_a]}$,

such that:

1) *(Timing) $t_{i,j}^l \leq t_{i,j}^b \leq t_{i,j}^e \leq t_{i,j}^r$ for all i, j, $t_{i,j+1}^l \geq t_{i,j}^r$ for all $j \in \mathbb{Z}_{[1,N_m-1]}$, $i \in \mathbb{Z}_{[1,N_a]}$, $t_{i,1}^l \geq T_0$, $t_{i,N_m}^r \leq T_f$, for all $i \in \mathbb{Z}_{[1,N_a]}$*
2) *(UAV trajectory) $x_a(t_{i,j}^l) = x_g(t_{i,j}^l)$, $\mathcal{E}(t_{i,j}^l) = 0$, $x_a(t_{i,j}^r) = x_g(t_{i,j}^r)$, $\mathcal{E}(t_{i,j}^r) \leq \mathcal{E}_{\max}$, for all $j \in \mathbb{Z}_{[1,N_m]}$, $i \in \mathbb{Z}_{[1,N_a]}$, and* (4) *is satisfied.*

3) *(Monitoring) for all $j \in \mathbb{Z}_{[1,N_m]}$, there exists $i \in \mathbb{Z}_{[1,N_a]}$ and $t^m_{i,j}$ such that $p_a^{(i)}(t) = p_m^{(j)}$, for all $t \in [t^b_{i,j}, t^e_{i,j}]$.*
4) *(UGV trajectory) $x_g(T_f) = x_{g,f}$ and (2), (6) are satisfied*

In Problem 1 the time instants $t^l_{i,j}$, $t^b_{i,j}$, $t^e_{i,j}$, $t^r_{i,j}$ are the launch, beginning of the monitoring, end of the monitoring and recovery time of UAV i to target j, respectively. For notational simplicity we determine such time instants for all UAVs to each target, but we only require *one* UAV to actually reach the target for monitoring, that means that the launch, monitoring (beginning and ending), and release time for all the others may be set equal, and hence ignored. We determine UAV commands only between launch and beginning of monitoring, and between end of monitoring and recovery. Between recovery and the next launch the UAVs will be docked with the UGV, and during monitoring the UAVs are considered stationary, though practically they will use a separate motion strategy to optimize data acquisition.

In practice, to solve Problem 1 as a whole may be challenging due to the different time-scales of UGV and UAVs motions, the hybrid nature of the decision variables, i.e., continuous control signals and discrete events such as launch and recovery, and the possibly large number of variables when many UAVs are considered. In what follows we develop a method to decouple the motion planning for UGV and UAVs while ensuring that recovery can be achieved within the UAV range and safe flight envelope.

III. Decoupling UGV and UAV planning using Reachable sets

In order to decouple the planning of UGV and UAVs we need to ensure that after launch from the UGV, the UAVs can accomplish their mission and return to the UGV within the available battery energy and flight envelope constraints. In what follows we focus on the recovery phase, when the UAV must rendezvous with the UGV, before its battery depletes. The method is also applicable to the launch phase, when the UAV reaches the target launching from the UGV, yet we focus on the recovery because then range is a critical constraint. In what follows we refer to a generic UAV and monitoring target, so we drop the indices i, j for simplicity.

As mentioned in Section II, the energy usage during flight is known fairly precisely[1], but during monitoring it is hard to predict. Thus, we determine the set of states that are reachable from a monitoring target position p_m, while satisfying flight envelope constraints, for a given return energy budget $\gamma_e < \mathcal{E}_{\max}$,

$$\begin{aligned}\mathcal{R}(p_m,\gamma_e) = \{\bar{x}_a \in \mathbb{R}^{n_a} : \exists t_f < \infty, u_a : [0,t_f] \to \mathbb{R}^m,\\ x_a(0) = (p_m,0), \mathcal{E}(0) = 0,\ x_a(t_f) = \bar{x}_a, \mathcal{E}(t_f) \le \gamma_e,\\ x_a(t) \in \mathcal{X}_a, u_a(t) \in \mathcal{U}_a, \forall t \in [0,t_f]\}.\end{aligned} \tag{7}$$

Then, by imposing the UGV position position constraint

$$(p_g(t),0) \in \mathcal{R}(p_m,\gamma_e), \forall t \in [t_1,t_2], \tag{8}$$

[1]It is precisely computed from data on aircraft's pilot operating handbook (POH) by the flight computer or manually using charts.

where $t_1, t_2 \in \mathbb{R}_+$ are given, we guarantee that if the UAV starts in an appropriate time interval and with remaining energy at least γ_e, it can execute a rendezvous trajectory from the monitoring target to a stationary flight at the UGV position.

The general reachable set (7) may be challenging to compute, and imposing the resulting constraint (8) in an optimal control problem may make its solution challenging. Thus, we build sets that are more conservative but easier to compute and use in optimization.

A. Reachable set construction

Reachability can be computed efficiently for several set classes, e.g., polyhedra, ellipsoids, zonotopes [9]–[11]. Ellipsoids have a compact representation as a single convex constraint, which makes them suitable for optimization. To implement (7) by ellipsoids, we consider a fixed linear UAV control law

$$u = K\delta x_a,\ \delta x_a = (x_a - x_s), \tag{9}$$

where $x_s = (p_s, 0)$ is the desired equilibrium, resulting in the asymptotically stable closed-loop dynamics

$$\delta\dot{x}_a(t) = (A + BK)\delta x_a = A_{cl}\delta x_a. \tag{10}$$

Constructing the reachable set proceeds in two steps: (i) building a stabilizing control law (9) and Lyapunov function $\mathcal{V}_c$ that results in a sublevel set $\mathcal{S}_c$ where the constraints are satisfied; (ii) building a Lyapunov function $\mathcal{V}_e$ that results in the reachable set within a given energy budget γ_e as a sublevel set $\mathcal{S}_e$ for the obtained closed-loop dynamics.

We construct and K in (9) such that the closed-loop (10) is exponentially stable and $\mathcal{V}_c(\delta x_a) = \delta x_a^\top P_c \delta x_a^\top$, $P_c \succ 0$ is a corresponding Lyapunov function (10),

$$\dot{\mathcal{V}}_c(\delta x_a(t)) \le -\alpha \mathcal{V}_c(\delta x_a(t)), \tag{11}$$

with a decay rate $\alpha \in \mathbb{R}_+$. P_c and K can be easily computed by a semidefinite program [12]. Let the sublevel set $\mathcal{S}_c = \{\delta x_a :\ \mathcal{V}_c(x_a) \le 1\}$ satisfy $\mathcal{S}_c \subseteq \{\delta x_a :\ \delta x_a \in \mathcal{X}_a,\ K\delta x_a \in \mathcal{U}_a\}$, then

$$\begin{aligned}\mathcal{R}_c(p_m) = \{x_a = (p_a,0) : (x - x_a)^\top P_c (x - x_a) \le 1,\\ x = (p_m,0)\},\end{aligned} \tag{12}$$

is the set of equilibria $(p_a, 0)$ that are reachable from initial state $(p_m, 0)$ by control law (9) without violating state or input constraints[2].

For computing the reachable set within a given energy budget, the energy consumed by the closed-loop dynamics (9) to reach a given equilibrium x_s from initial state x_a is

$$\mathcal{V}_e(\delta x_a) = \int_0^\infty \dot{\mathcal{E}}(t)dt \le \gamma_e. \tag{13}$$

Then, the sublevel set $\mathcal{S}_e = \{\delta x_a :\ \mathcal{V}_e(\delta x_a) \le \gamma_e\}$ includes trajectories with energy usage less than γ_e. It is

[2]The constraint sets $\mathcal{X}_a$, $\mathcal{U}_a$ do not change when considering the error state δx_a because they do not include constraints on position. Otherwise, an augmented state vector will be needed.

straightforward that for (5), (10), $\mathcal{V}_e(\delta x_a) = \delta x_a^\top P_e \delta x_a$ where $P_e \succ 0$ is the solution of $P_e(A+BK) + (A+BK)^\top P_e = -(Q_e + K^\top R_e K)$. Thus,

$$\mathcal{R}_e(p_m, \gamma_e) = \{x_a = (p_a, 0) : (x - x_a)^\top P_e (x - x_a) \leq \gamma_e, \\ x = (p_m, 0)\}, \tag{14}$$

is the set of equilibria reached from initial state $(p_m, 0)$ by control law (9) with energy expenditure less than γ_e.

Finally, consider the set

$$\mathcal{R}_K(p_m, \gamma_e) = \mathcal{R}_e(p_m, \gamma_e) \cap \mathcal{R}_c(p_m), \tag{15}$$

which is invariant, since for any $\delta x_a \in \mathcal{S}_c \cap \mathcal{S}_e$, $\mathcal{V}_c(A_{cl}\delta x_a) \leq \mathcal{V}_c(\delta x_a)$, and $\mathcal{V}_e(A_{cl}\delta x_a) \leq \mathcal{V}_e(\delta x_a)$ due to the integral in (13), so that $A_{cl}\delta x_a \in \mathcal{R}_e(p_m, \gamma_e) \cap \mathcal{R}_c(p_m)$. Then, the constraint

$$(p_g, 0) \in \mathcal{R}_K(p_m, \gamma_e), \tag{16}$$

determines a set of rendezvous positions for the UAV with the UGV, such that the UAV trajectories from stationary flight at the monitoring target position p_m to equilibria in such positions satisfy flight envelope constraints and energy budget. In (16) we consider only the rendezvous position and ignore velocity, as the UGV velocity may briefly stop to allow landing, or the UAV may simply perform a landing on a (slowly) moving platform.

Using the exponential stability of $\mathcal{V}_c$ from (11), we can bound the time for the UAV to reach a neighborhood of the equilibrium, where the rendezvous occurs. Since $\delta x_a(t)^\top P_c \delta x_a(t) \leq 1$ for all $t \in \mathbb{R}_{0+}$, $\mathcal{V}_c(\delta x_a(t)) \leq \mathcal{V}_c(\delta x_a(0))e^{-\alpha t} \leq e^{-\alpha t}$. Then, for any $\epsilon \in \mathbb{R}_{(0,1)}$

$$T_{\text{rec}} = -\alpha^{-1} \ln \epsilon, \tag{17}$$

is the upper bound to the time to achieve $\mathcal{V}_c(\delta x_a) \leq \epsilon$, that defines the acceptable rendezvous region for ϵ small enough.

IV. Trajectory optimization for UGV

Leveraging the reachable set constraints (16) developed in Section III, we can formulate the UGV trajectory generation separately from the UAVs, while ensuring that rendezvous can occur within the range constraints.

As UGV model (1), we use the kinematic bicycle model

$$\dot{p}_g^x = v_g \cos\theta_g \tag{18a}$$
$$\dot{p}_g^y = v_g \sin\theta_g \tag{18b}$$
$$\dot{\theta}_g = \frac{v_g \tan(\delta_g)}{L} \tag{18c}$$
$$\dot{v}_g = a_g, \tag{18d}$$

where (p_g^x, p_g^y) is the position, θ_g is the yaw angle, v_g is the velocity, a_g is the acceleration, δ_g is the front-steering angle, and L is the wheelbase. The state and input vectors are $x_g = [p_g^x, p_g^y, \theta_g, v_g]^\top$, $u_g = [a_g, \delta_g]^\top$, respectively.

For the UGV constraints (2), we consider

$$\mathcal{X}_g = \{x_g : 0 \leq v_g \leq v_{g\max}\}, \tag{19a}$$
$$\mathcal{U}_g = \{u_g : |a_g| \leq a_{g\max}, |\delta_g| \leq \delta_{g\max}\}. \tag{19b}$$

The achievable rendezvous constraint that enforces the UGV to remain inside the reachable set $\mathcal{R}_K(p_m, \gamma_e)$ of the UAV for a time interval is

$$\exists t_1^{(j)}, t_2^{(j)} \in [T_0, T_f] \quad \text{s.t.} \quad (p_g(t), 0) \in \mathcal{R}_K(p_m^{(j)}, \gamma_e^{(j)}), \\ \gamma_e^{(j)} \leq \gamma_{\max}, t_2^{(j)} - t_1^{(j)} \geq T_{\min}, \forall t \in [t_1^{(j)}, t_2^{(j)}], \tag{20}$$

where $T_{\min} \in \mathbb{R}_+$ is the minimum duration of the rendezvous window. The upper bound to the energy budget for rendezvous $\gamma_{\max} < \mathcal{E}_{\max}/2$ is chosen to leave enough energy for launch and monitoring.

Summarizing, the free-final-time optimal trajectory generation problem for the UGV that ensures feasibility of the rendezvous is formulated as

$$\max_{u_g(\cdot), \gamma_e^{(j)}, T_f} \int_{T_0}^{T_f} J(x_g(t), u_g(t))\mathrm{d}t + w_{g\gamma} \sum_{j=1}^{N_m} \gamma_e^{(j)} \tag{21a}$$
$$\text{s.t. } (18), (19), (6), (20),\ j \in \mathbb{Z}_{[1,N_m]}, \tag{21b}$$
$$x_g(T_0) = x_{g,s},\ x_g(T_f) = x_{g,f}. \tag{21c}$$

The cost function $J : \mathbb{R}^{n_g} \times \mathbb{R}^{m_g} \to \mathbb{R}$ includes the completion, i.e., final, time and the input energy,

$$J(x_g) = w_{gt} + w_{ge} u_g^\top u_g,$$

where $w_{gt},\ w_{ge},\ w_{g\gamma} \in \mathbb{R}_+$ are user-defined weights.

In order to solve (21b) numerically, we discretize it with time scaling. We use a multiple shooting parameterization [13] with the adaptive time-mesh

$$T_0 = t_0 < t_1 < \cdots < t_N = T_f,$$

where $N \in \mathbb{N}$ is the number of sub-intervals $[t_k, t_{k+1}]$ for $k \in \mathbb{Z}_{[0,N-1]}$, and we introduce time-scaling variables

$$s_k = t_{k+1} - t_k. \tag{22}$$

By parametrizing the control as a first order hold and integrating in the intervals, the dynamics are

$$x_{k+1} = f_g^{(d)}(x_k, u_k, u_{k+1}, s_k). \tag{23}$$

and the constraints (2), (6) are enforced at node points,

$$x_k \in \mathcal{X}_g, \quad u_k \in \mathcal{U}_g, \quad p_{g,k} = h_g(x_k, u_k) \notin \mathcal{O}^{(o)}, \tag{24}$$

where $x_k \triangleq x_g(t_k)$, $u_k \triangleq u_g(t_k)$, To implement the rendezvous constraint (20), we first assign consecutive node points $\{k_1^{(j)}, k_1^{(j)}+1, \ldots, k_2^{(j)}\}$ to each monitoring target $j \in \mathbb{Z}_{[1,N_m]}$. Then, we formulate (20) as

$$\sum_{k=k_1^{(j)}}^{k_2^{(j)}-1} s_k \geq T_{\min},\ \gamma_e^{(j)} \leq \gamma_{max}, \\ (p_{g,k}, 0) \in \mathcal{R}_K(p_m^{(j)}, \gamma_e^{(j)}), \quad k \in \mathbb{Z}_{[k_1^{(j)}, k_2^{(j)}]}. \tag{25}$$

In (20), even if $k_1^{(j)}$, $k_2^{(j)}$ are specified, the time instants $t_1^{(j)}$ and $t_2^{(j)}$ are not fixed, since s_k is a decision variable.

Thus, the discrete-time formulation of (21) is

$$\max_{u_k, s_k, \{\gamma_e^{(j)}\}_j} \quad w_{gt} \sum_{k=0}^{N-1} s_k + w_{ge} \sum_{k=0}^{N} u_k^\top u_k + w_{g\gamma} \sum_{j=1}^{N_m} \gamma_e^{(j)} \tag{26a}$$

$$\text{s.t. (23) (24)} \tag{26b}$$

$$(25),\ k \in \mathbb{Z}_{[k_1^{(j)}, k_2^{(j)}]},\ j \in \mathbb{Z}_{[1, N_m]}, \tag{26c}$$

$$x_0 = x_{g,s},\ x_N = x_{g,f}. \tag{26d}$$

which can be solved by algorithms such as [14].

V. Launch and Recovery Trajectory Optimization for UAVs

Besides for generating the UAV recovery trajectories, the control law (9) in Section III can be used to compute the launch instants and launch trajectories, by defining the energy budget to travel to the target and using the monitoring target position $p_m^{(j)}$ as equilibrium of the Lyapunov function. However, we see that as less critical because at launch the UAVs have full energy.

In practice, it is convenient to further optimize both launch and recovery the UAV trajectories which provide additional time/energy for the monitoring activities, and/or less time for re-charging at the UGV. Thus, we formulate optimal control problems for launch and recovery that are guaranteed to be feasible since (16) holds the trajectory generated by (9) is feasible, and it can be used both as initial guess and as backup, should the optimization not converge in the available time or encounter numerical issues.

A. Optimization of UAV recovery trajectory

The recovery trajectory planning computes the trajectory of the UAV for returning to the UGV from the monitoring target position. Due to the construction in Section III such trajectory can be generated easily using the linear control law (9). Let $t_{i,j}^r \in [t_1^{(j)}, t_2^{(j)}]$, where $t_1^{(j)}, t_2^{(j)}$ are as in (20), the recovery trajectory is generated as the output of

$$\dot{x}_a^{(i)}(t) = (A + BK)x_a^{(i)}(t) - BK(p_g(t_{i,j}^r), 0) \tag{27a}$$

$$u_a^{(i)}(t) = BK(x_a^{(i)}(t) - (p_g(t_{i,j}^r), 0)) \tag{27b}$$

$$x_a^{(j)}(t_{i,j}^e) = (p_m^{(j)}, 0) \tag{27c}$$

until $t = t_{i,j}^r$, where $t_{i,j}^e = t_{i,j}^r - T_{\text{rec}}$ is computed according to (17). The monitoring operation continues until either $t < t_{i,j}^e$ or the remaining energy reaches $\gamma_e^{(j)}$, where, if the latter occurs sooner than the former, the UAV hovers until $t_{i,j}^e$ at the monitoring target, or starts the return trajectory earlier than $t_{i,j}^e$ and hovers, or wait on the ground, at the rendezvous location $p_g(t_{i,j}^r)$.

Due to the construction of the control law (9) and imposing of constraint (20) on the UGV, the recovery trajectory is guaranteed to achieve the rendezvous condition $\mathcal{V}_c(x_a - (p_g, 0)) \leq \epsilon$, while satisfying the flight envelope constraints and within the energy budget $\gamma_e^{(j)}$.

Further optimization of the recovery trajectory can be achieved to possibly delaying the departure time and/or minimizing the used energy, hence leaving more time/energy for the monitoring operation. We can generate the optimized trajectory by solving

$$\min_{u_a(t), \tilde{t}_{i,j}^e} \quad -w_t^r \tilde{t}_{i,j}^e + w_e^r \mathcal{E}(t_{i,j}^r) \tag{28a}$$

$$\text{s.t.} \quad \tilde{t}^e \geq t^e \tag{28b}$$

$$(3), (4), (5) \tag{28c}$$

$$x_a^{(i)}(\tilde{t}^e) = (p_m^{(j)}, 0) \tag{28d}$$

$$\mathcal{V}_c(x_a^{(i)}(t_{i,j}^r) - x_g(t_{i,j}^r)) \leq \epsilon \tag{28e}$$

$$\mathcal{E}(\tilde{t}_{i,j}^e) = 0, \quad \mathcal{E}(t_{i,j}^r) \leq \gamma_e^{(j)}, \tag{28f}$$

where $w_t^r, w_e^r \in \mathbb{R}_{++}$ are user-defined weights. Problem (28) is guaranteed to be feasible because the solution from (27) is feasible, with $\tilde{t}_{i,j}^e = t_{i,j}^e$. With the newly computed departure time $\tilde{t}^e$ and energy $\mathcal{E}(t^r)$, the UAV can operate for longer at the monitoring location.

B. Optimization of UAV launch trajectory

The launch trajectory for the UAV starts from the UGV position p_g, reaches the target position $p_m^{(j)}$ and its energy usage must be smaller than $\mathcal{E}_{\max} - \gamma_{\max}$, to save some energy for monitoring. This may be achieved by choosing t^l to avoid releasing the UAV when too far from target, e.g., according to the scenario and UGV trajectory, or by the results of Section III.

Given the launch time $t_{i,j}^l$, the optimization of the launch trajectory is formulated as

$$\min_{x_a(\cdot), u_a(\cdot), t_{i,j}^b} \quad w_t^l t_{i,j}^b + w_e^l \int_{t^l}^{t^b} \dot{\mathcal{E}}(t) \mathrm{d}t \tag{29a}$$

$$\text{s.t. } (3), (4), \tag{29b}$$

$$x_a(t_{i,j}^l) = (p_g(t_{i,j}^l), v(t_{i,j}^l)), \tag{29c}$$

$$x_a(t_{i,j}^b) = (p_m^{(j)}, 0), \tag{29d}$$

where $v = (v_g \sin\theta_g, v_g \cos\theta_g)$ is the UGV velocity vector. The cost function (29a) aims at minimizing the flight time and the energy with user-defined weights $w_t^l, w_e^l \in \mathbb{R}_+$. The problem in (29) is a free-final-time optimal control problem subject to convex state and input constraints.

C. Trajectory generation and execution summary

The approach for solving the UGV-UAVs trajectory generation Problem 1 with the method proposed in this paper and the execution of the UGV and UAVs trajectories is summarized in Algorithm 1.

VI. Case Study

We consider a case study for validating the proposed method, where we use the following parameters:

$$\begin{gathered} c_1 = 0.2, c_2 = 1, \alpha = 0.025, \epsilon = 10^{-4}, \\ v_{\max} = 25\text{m/s}, a_{\max} = 10\text{m/s}^2, \gamma_{\max} = 6000, \\ T_{\min} = 600\text{s}, w_{gt} = 1, w_{ge} = 0.02, w_{g\gamma} = 200, \\ w_t^r = 1, w_e^r = 0.1, w_t^l = 1, w_e^l = 0, L = 2, N = 34, \\ v_{g\max} = 10\text{m/s}, a_{g\max} = 1\text{m/s}^2, \delta_{g\max} = 5\text{deg}. \end{gathered}$$

Algorithm 1 Decoupled UGV and UAVs Trajectory Planning

Parameters: $\gamma_{\max}, c_1, c_2, \mathcal{X}_g, \mathcal{U}_g, \mathcal{X}_a, \mathcal{U}_a$

Data: $p_m^{(j)}$ for all $j \in \mathbb{Z}_{[0,N_m]}$, $\mathcal{O}^{(o)}$, for all $o \in \mathbb{Z}_{[0,N_o]}$, $x_{g,f}$, T_0, $x_g(T_0) = x_a^{(i)}(T_0) = x_{g,s}$ for all $i \in \mathbb{Z}_{[0,N_a]}$,

Trajectory Generation:

Construct $\mathcal{R}_K, T_{\mathrm{rec}}, K$ by (15),(17)
Compute T_f, $\gamma_e^{(j)}$, $t_{i,j}^r$ for all $j \in \mathbb{Z}_{[1,N_m]}$, $i \in \mathbb{Z}_{[1,N_a]}$, $(x_g(t), u_g(t))$ by (21) for $t \in [T_0, T_f]$
Compute updated $\gamma_e^{(j)}$, $t_{i,j}^e$ and $(x_a^{(i)}(t), u_a^{(i)}(t))$ for $t \in [t_{i,j}^e, t_{i,j}^r]$, for all $j \in \mathbb{Z}_{[1,N_m]}$, $i \in \mathbb{Z}_{[1,N_a]}$ by (28)
Compute $t_{i,j}^l$, $t_{i,j}^b$ and $(x_a^{(i)}(t), u_a^{(i)}(t))$ for $t \in [t_{i,j}^l, t_{i,j}^b]$, for all $j \in \mathbb{Z}_{[1,N_m]}$, $i \in \mathbb{Z}_{[1,N_a]}$ by (29)

Trajectory Execution:

Execute UGV trajectory $x_g(t)$ for $t \in [T_0, T_f)$
for $i = 1 : N_a$ **do**
  for $j = 1 : N_m$ **do**
    Launch UAV i to target j at $t_{i,j}^l$ and execute $x_a^{(i)}(t)$ for $t \in [t_{i,j}^l, t_{i,j}^b]$
    while $t \in [t_{i,j}^l, t_{i,j}^b[$ **and** $\mathcal{E}^{(i)} \leq \mathcal{E}_{\max} - \gamma_e^{(j)}$ **do**
      Monitor target j with UAV i
    end while
    Return UAV i to UGV by $x_a^{(i)}(t)$ for $t \in [t_{i,j}^e, t_{i,j}^r]$
  end for
end for

We construct the sets using MOSEK to obtain P_c and K, and solve the optimal trajectory generation for UGV (26) and UAVs (28), (29) by the PTR method [15] using GUROBI from MATLAB. The computation of the UGV trajectory from (26) takes less than 6s and the computation of the optimized recovery and launch trajectories from (28) and (29), respectively, take less than 0.5s on an 2023 14" MacBook Pro M2 laptop with 64GB Ram running Matlab 2021b (non-native for M2).

The reachable set $\mathcal{R}_K$ of the UAV is shown in Fig. 2, where we confirm the constraint satisfaction of the reachable set by showing the projections of $\mathcal{R}_c$ in the velocity and acceleration planes. Fig. 2 also shows the recovery trajectory by linear control (27) and the optimized one (28) with the highlighted corresponding linear (T_{rec}) and optimized ($\tilde{T}_{\mathrm{rec}}$) recovery instants. The comparisons between energy consumption of linear (27) and optimal (28) recovery trajectory are obtained from an initial point on the border of $\mathcal{R}_K$. Clearly, the energy consumption and the recovery time $\tilde{T}_{\mathrm{rec}}$ are improved by the refinements in Section V, which provides longer time for monitoring, or a shorter re-charge period at the UGV carrier.

Fig. 3 shows the results for the UGV trajectory, where the optimized completion time is $T_f = 105\text{m}, 47\text{s}$. In the environment, there are 18 monitoring targets ($N_m = 18$), clustered in groups of at most 5, which determines the maximum number of UAVs operating concurrently, and 3 ellipsoidal obstacles ($N_o = 3$). For the rendezvous constraint (25), we specify $(k_1^{(j)}, k_2^{(j)})$ such that $k_2^i - k_1^i = 2$, i.e., three

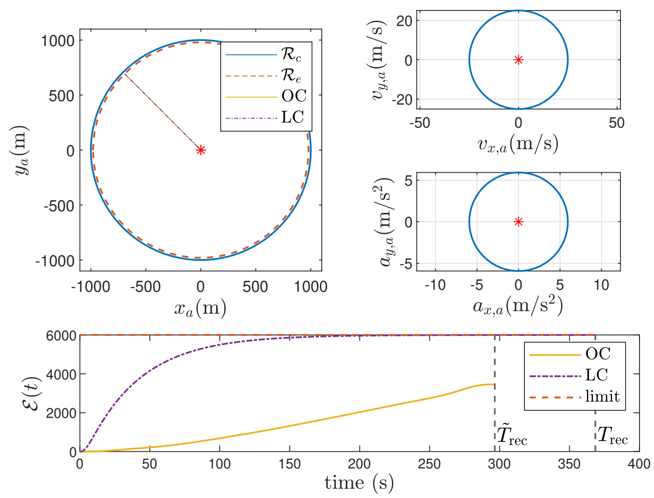

Fig. 2. Reachable set $\mathcal{R}_K$ of the UAV. Top left: constrained feasible set $\mathcal{R}_c(0)$, energy bound set $\mathcal{R}_e(0, \gamma_{\max})$ and recovery trajectories computed from linear control (LC) and optimal control (OC). Top right, middle right: $\mathcal{R}_c$ projected onto the velocity and acceleration planes, respectively. Bottom: cumulative energy consumption for LC and OC trajectory, and corresponding recovery trajectory durations T_{rec}, $\tilde{T}_{\mathrm{rec}}$.

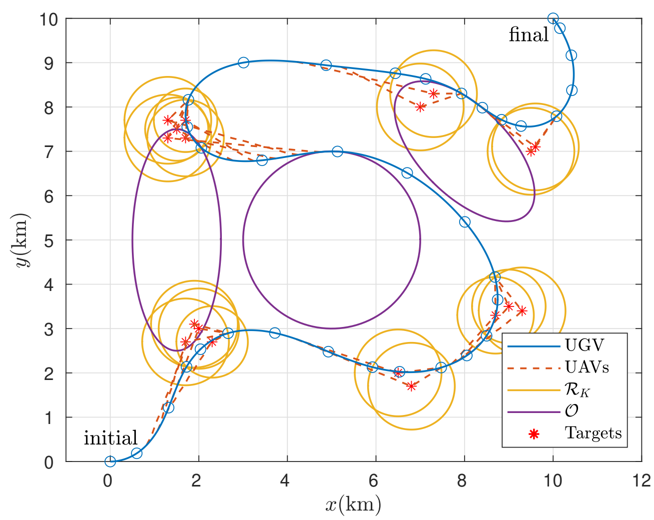

Fig. 3. Trajectories of UGV and UAVs. Circular markers on the trajectory of the UGV represent node points.

consecutive nodes are assigned to each target j in $\mathbb{Z}_{[1,N_m]}$, and hence two arcs of the UGV trajectory remain within the set $\mathcal{R}_K$ centered at the target, see in Fig. 3.

The launch and recovery trajectories of the UAVs are also shown in Fig. 3. While in an actual mission the end time of monitoring t^e varies due to factors such as acquired information and remaining energy, in the simulations t^e is such that the rendezvous time t^r occurs when the UGV is at the exiting border of the $\mathcal{R}_K$ sets, i.e., t_2 in (20). This allows the UAV to stay the longest at the monitoring target. Fig. 3 shows that rendezvous always occur in the reachable sets of the UAV, and hence, according to Fig. 2, flight envelope and range constraints are satisfied. Fig. 4 shows some zoomed-in views of the operations for two targets, and

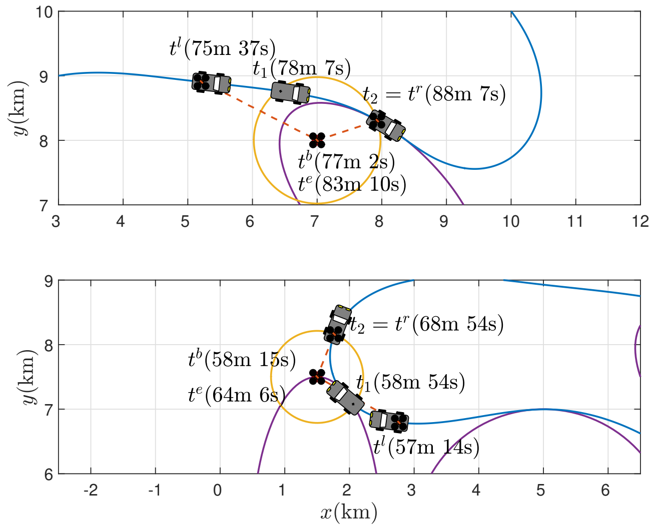

Fig. 4. Zoom-in on parts of Fig. 3. Monitoring missions for two targets, with the corresponding UGV and UAVs trajectories and time instants $t^l, t^b, t^e, t^r, t_1, t_2$.

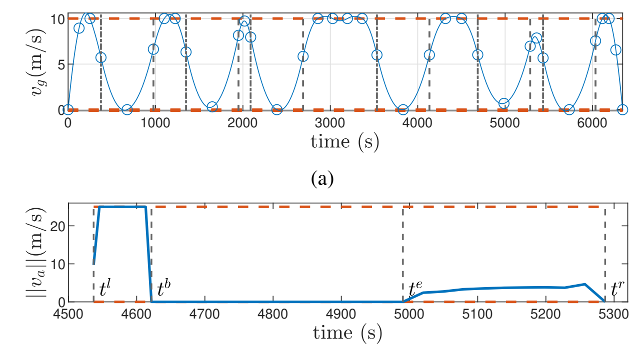

Fig. 5. (a) Time history of the UGV velocity (blue) during the entire trajectory shown in Fig. 3, velocity constraints (red dash), discretization nodes (circles), $t_1^{(j)}$ (dot-dash), $t_2^{(j)}$ (dash). (b) Time history of the UAV velocity vector norm (blue) during the monitoring mission shown in Fig. 4-top, and velocity constraints (red dash).

the corresponding time instants $t^l, t^b, t^e, t^r, t_1, t_2$. Fig. 5(a) shows that the velocity of the UGV satisfies constraints at nodes, yet small violations may occur between nodes, which may be removed by the method in [16]. Fig. 5(b) shows the norm of the velocity vector of the UAVs during an entire monitoring mission for a single target, including launch, monitoring, and recovery. For the launch trajectory, the primary objective is to minimize the time, while for the recovery trajectory, the primary objective is to minimize the energy usage. During monitoring, the UAV is shown as stationary, though in reality it will move with a separated strategy to optimize information acquisition, which further motivates the setting of an energy recovery budget, to trigger the return to the UGV.

VII. Conclusions

We have presented a method for generating trajectories for a UGV carrying multiple UAVs for monitoring tasks that allows for decoupling UGV and UAVs planning, while guaranteeing recovery satisfying flight envelope and energy range constraints. The method uses Lyapunov functions to build reachable sets where the constraints are satisfied, and then use those within the UGV trajectory generation problem to ensure feasibility of UAVs rendezvous, possibly extended to launch. The method provides candidate UAV trajectories for recovery and launch, which may be improved by optimal trajectory generation. Future works will consider the recharge period and possibly modifications to the monitoring targets sequence to further optimize the overall mission, the usage of different sets for reachability, and the optimization of motion for information acquisition during monitoring [17].

References

[1] M. Dunbabin and L. Marques, "Robots for environmental monitoring: Significant advancements and applications," *IEEE Robotics & Automation Mag.*, vol. 19, no. 1, pp. 24–39, 2012.

[2] P. Thaker, S. Di Cairano, and A. P. Vinod, "Bandit-based multi-agent search under noisy observations," in *Proc. IFAC World Congress*, 2023.

[3] Y. Ding, B. Xin, and J. Chen, "A review of recent advances in coordination between unmanned aerial and ground vehicles," *Unmanned Systems*, vol. 9, no. 02, pp. 97–117, 2021.

[4] N. Mathew, S. L. Smith, and S. L. Waslander, "Multirobot rendezvous planning for recharging in persistent tasks," *IEEE Tr. Robotics*, vol. 31, no. 1, pp. 128–142, 2015.

[5] K. Yu, A. K. Budhiraja, and P. Tokekar, "Algorithms for routing of unmanned aerial vehicles with mobile recharging stations," in *2018 IEEE int. conf. robot. aut.*, 2018, pp. 5720–5725.

[6] K. Yu, A. K. Budhiraja, S. Buebel, and P. Tokekar, "Algorithms and experiments on routing of unmanned aerial vehicles with mobile recharging stations," *J. Field Rob.*, vol. 36, no. 3, pp. 602–616, 2019.

[7] M. Won, "Ubat: On jointly optimizing uav trajectories and placement of battery swap stations," in *IEEE Int. Conf. Robot. Aut.*, 2020.

[8] F. Blanchini and S. Miani, *Set-theoretic methods in control*. Springer, 2008.

[9] F. Borrelli, A. Bemporad, and M. Morari, *Predictive control for linear and hybrid systems*. Cambridge University Press, 2017.

[10] A. B. Kurzhanski and P. Varaiya, "Ellipsoidal techniques for reachability analysis," in *Hybrid Systems: Comp. Control*. Springer, 2000.

[11] A. Girard, "Reachability of uncertain linear systems using zonotopes," in *Hybrid Systems: Computation and Control*, 2005, pp. 291–305.

[12] T. Kim, P. Elango, T. P. Reynolds, B. Açıkmeşe, and M. Mesbahi, "Optimization-based constrained funnel synthesis for systems with lipschitz nonlinearities via numerical optimal control," *IEEE Control Systems Letters*, vol. 7, pp. 2875–2880, 2023.

[13] H. G. Bock and K.-J. Plitt, "A multiple shooting algorithm for direct solution of optimal control problems," in *Pr. IFAC World Cong.*, 1984.

[14] A. G. Kamath, P. Elango, Y. Yu, S. Mceowen, J. M. Carson III, and B. Açıkmeşe, "Real-time sequential conic optimization for multi-phase rocket landing guidance," *arXiv preprint arXiv:2212.00375*, 2022.

[15] T. P. Reynolds, M. Szmuk, D. Malyuta, M. Mesbahi, B. Açıkmeşe, and J. M. Carson III, "Dual quaternion-based powered descent guidance with state-triggered constraints," *J. Guidance, Control, and Dynamics*, vol. 43, no. 9, pp. 1584–1599, 2020.

[16] K. Teo and C. Goh, "A simple computational procedure for optimization problems with functional inequality constraints," *IEEE Tr. Automatic Control*, vol. 32, no. 10, pp. 940–941, 1987.

[17] A. D. Bonzanini, A. Mesbah, and S. Di Cairano, "Perception-aware model predictive control for constrained control in unknown environments," *Automatica*, 2024, to appear.